Research Square

Preprints are preliminary reports that have not undergone peer review.
They should not be considered conclusive, used to inform clinical practice,
or referenced by the media as validated information.

Modelling Daily Maximum Temperature Extremes in Namibia Using Extreme Value Theory

SM Nuugulu

snuugulu@unam.na

University of Namibia

MS Mandume

University of Namibia

A Shikongo

University of Namibia

Research Article

Keywords:

Posted Date: November 26th, 2026

DOI: https://doi.org/10.21203/rs.3.rs-11555426/v1

License: This work is licensed under a Creative Commons Attribution 4.0 International License.
Read Full License

Additional Declarations: No competing interests reported.

Modelling Daily Maximum Temperature Extremes in Namibia Using Extreme Value Theory

S.M. Nuugulu[a,*], M.S. Mandume[a], A. Shikongo[b]

[a]*Department of Computing, Mathematical and Statistical Sciences, University of Namibia, Windhoek, Namibia*
[b]*School of Engineering and the Built Environment, JEDS Campus, University of Namibia, Namibia*

Abstract

Extreme temperatures, including severe heat events, pose substantial risks to human health, infrastructure, water resources, agriculture, and other climate-sensitive sectors. In Namibia, recurrent periods of intense heat highlight the need for robust statistical approaches for quantifying the frequency and magnitude of extreme temperature events. This study applies Extreme Value Theory (EVT) to characterise extreme daily maximum temperatures at three meteorological stations in Namibia using two complementary approaches: the Block Maxima (BM) method based on the Generalized Extreme Value (GEV) distribution and the Peaks Over Threshold (POT) method based on the Generalized Pareto Distribution (GPD). The analysis uses 29 044 daily maximum temperature observations recorded between 1990 and 2019 by the Namibia Meteorological Services (NMS). Under the BM approach, annual maximum temperatures are modelled using the GEV distribution, while the POT approach uses station-specific thresholds selected through mean residual life, parameter stability, and exceedance diagnostics. Model parameters are estimated using maximum likelihood estimation (MLE), and performance of the model is assessed through graphical diagnostics and empirical goodness-of-fit measures. Bootstrap procedures are further employed to quantify uncertainty in GPD parameter estimates and return levels. The results demonstrate substantial spatial variation in extreme-temperature behaviour across the three stations. The GPD shape estimates are negative for all stations, indicating bounded upper-tail behaviour, while the estimated 100-year POT return levels range from 38.82°C at Windhoek to 43.67°C at Walvis Bay. The comparison of the GEV and GPD further demonstrates the importance of model choice when quantifying rare temperature events. The findings further provide station-specific estimates of extreme-temperature risk and a statistical basis for heat-risk assessment, early-warning systems, climate adaptation, and long-term planning in Namibia.

Keywords: Extreme Value Theory (EVT), Block Maxima (BM), Peaks Over Threshold (POT) , Extreme Temperature, Generalized Extreme Value Distribution (GEV), Generalized Pareto Distribution (GPD), Return Levels, Namibia

1. Introduction

Climate change has increased the frequency, intensity, and duration of extreme weather and climate events in many regions of the world, making them one of the most pressing environmental challenges of the twenty-first century [1]. Among these events, extreme temperature events, particularly extreme high temperatures, have attracted intense scientific attention because of their far-reaching consequences for human health, agriculture, water resources, ecosystems, infrastructure,

*Corresponding author.
Email address: snuugulu@unam.na, tell: +26461 206 3961 (S.M. Nuugulu)

energy consumption and broader socioeconomic development [2, 3]. Unlike average climatic conditions, temperature extremes tend to cause severe impacts, such as substantial economic losses, reduced agricultural productivity, higher mortality, and increased strain on critical infrastructure and public services [2, 4]. A proper understanding of the statistical behaviour of temperature extremes is essential for assessing climate risks, disaster preparedness, and the formulation of effective adaptation and mitigation strategies.

Although scientific evidence indicates that human activities are often the main drivers of climate change, its full scope and consequences are poorly understood. The consequences resulting from extremely high temperatures are more evident in areas that have arid or semi-arid climates because their natural variability is quite high and adaptation is not always easy [3, 5]. Namibia, one of the dry nations in Sub-Saharan Africa, is especially vulnerable to climate variability due to its arid climate, limited and unpredictable rainfall, and heavy reliance on climate-sensitive sectors such as agriculture, livestock production, water, biodiversity, and tourism [5, 6]. The national climate is strongly shaped by the cold Benguela Current along the Atlantic coast, the subtropical high-pressure system, and regional atmospheric circulation patterns, all of which contribute to considerable spatial and temporal variability in temperature [8, 7]. Central and coastal regions, such as Walvis Bay, are particularly vulnerable, with exceptionally high temperature events becoming increasingly frequent and clearly evident in recent years, sparking growing concern over food security, water availability, ecosystem resilience, and sustainable economic development [3]. These mounting challenges highlight the urgent need for robust statistical methods capable of accurately characterizing both the occurrence and severity of extreme temperature events. One of such statistical approaches is Extreme Value Theory (EVT), which is specifically designed to analyze rare and extreme events.

Extreme Value Theory (EVT) provides a rigorous probabilistic model to study rare and extreme events by focusing on the probabilistic behavior of distribution tails rather than on average or typical outcomes [10, 9]. Fisher and Tippett [9] established the theoretical foundations of EVT demonstrating that extreme limit distributions fall into only one of three types: Gumbel, Fréchet, or Weibull. Each of these distributions exhibits distinct tail behaviors. Specifically, the Fréchet distribution is associated with long tails, the Weibull distribution with short tails, and the Gumbel distribution with light or medium tails. In contrast to classical statistical approaches that primarily describe average conditions, EVT is expressly designed to estimate the likelihood of events that occur infrequently but may have severe consequences than previously observed. Several studies have used extreme value theory (EVT) in various contexts to quantify both the frequency and severity of temperature extremes [3, 4, 10, 11]. In [10], recent methodological advances in extreme-value modelling of heatwaves explicitly account for both temporal persistence and spatial extent, addressing the limitations of traditional EVT approaches that focus only on intensity. Such spatio-temporal models have been shown to improve risk quantification for events such as the 2003 European heatwave, which caused tens of thousands of excess deaths and substantial agricultural losses [10]. The application of EVT extends beyond environmental and climate studies. For example, Wu et al. [12] used EVT to model the low-carbon development paths of freight enterprises, showing how the likelihood of adopting low-carbon behaviours varies with the stage of enterprise development and regional economic conditions. The theory has also been used widely in fields such as finance [13, 14, 15] and engineering [16] due to its ability to provide estimates on return levels, return periods, exceedance probability, and other metrics that are essential in uncertainty-based decision-making.

The two principal approaches used in EVT are the Block Maxima (BM) and the Peaks Over Threshold (POT) method. The BM approach divides the data into blocks and models the maximum values using the Generalized Extreme Value (GEV) distribution, while the POT approach models threshold exceedances using the Generalized Pareto Distribution (GPD) [4, 9, 10, 14, 16, 17, 18, 19]. These approaches have been successfully applied to analyse a wide range of environmental hazards, including extreme temperature, precipitation, floods, droughts, wind speeds, storm surges,

and many others [18, 19]. Their flexibility and strong theoretical foundation have made them the preferred statistical methodological approaches for analysing climatic extremes. For example, Lazoglou and Anagnostopoulou [18] applied EVT to data from ten meteorological stations across the Mediterranean, using both the BM and POT approaches and their results indicated that the Generalized Pareto Distribution (GPD) offered stronger theoretical justification than the Generalized Extreme Value (GEV) distribution for predicting extreme precipitation. More recent methodological work has also employed GEV and GPD models to investigate extreme temperatures, estimate return levels, and quantify climate-related risks across diverse climatic regions [20, 21, 22, 23]. In [20] BM approach was used to analyse the maximum summer temperatures, finding that the Weibull distribution provided the most appropriate fit. Some developments have extended classical EVT to non-stationary, Bayesian, spatial, and covariate-dependent approaches that enable researchers to incorporate climate trends, spatial dependence, and atmospheric drivers into extreme value analyses [24]. Although these methodological advances have considerably improved the understanding of climate extremes, the majority of existing studies have focused on Europe, North America, Asia, and selected regions of Africa, with relatively limited attention devoted to Namibia and other parts of Southern Africa [6].

In Namibia, previous climate studies have concentrated mainly on describing historical climate variability, drought occurrence, rainfall patterns, wind speed, and long-term temperature trends [6, 7, 8, 25]. Although these studies have provided valuable insights into the evolving climate of the country, none have yet employed Extreme Value Theory to probabilistically characterise extreme temperatures, estimate return levels, or systematically compare the performance of BM and POT approaches to model extreme temperatures in this setting. Consequently, limited data on the occurrence and frequency of temperature extremes hinder evidence-based climate adaptation, infrastructure development, disaster risk reduction, and policymaking.

This study seeks to address this gap by applying the Generalized Extreme Value (GEV) and Generalized Pareto Distribution (GPD) models to analyse daily maximum temperature extremes in Namibia. Although many previous studies have simply performed descriptive analyses of temperature variability, this study provides a probabilistic assessment of extreme temperatures through the estimation of return levels and return periods using both the Block Maxima and Peaks Over Threshold approaches. The comparison of these complementary EVT approaches provides additional insight into their suitability for modelling temperature extremes under Namibia's climatic conditions and contributes to a more comprehensive understanding of extreme temperature behaviour. The findings of this study can be used quantitatively for climate risk assessment, environmental planning, engineering designs, agricultural planning, and climate adaptation studies in Namibia. In addition, the study contributes to the growing body of literature on the application of Extreme Value Theory to climate extremes in areas where data is sparse and provides a statistical foundation for future research on non-stationary extreme value modelling, climate change attribution, and regional climate risk assessment.

2. Methodology

This study employs a quantitative research approach to model extreme high-temperature events in Namibia using the statistical model of Extreme Value Theory (EVT). In this study, two complementary EVT approaches are considered, namely the Block Maxima (BM) approach and the Peaks Over Threshold (POT) approach. The BM approach models annual maximum temperatures using the Generalized Extreme Value (GEV) distribution, while the POT approach models threshold exceedances using the Generalized Pareto Distribution (GPD). These approaches allow for the estimation of return levels, return periods, and the probability of future extreme temperature events. The methodology consists of six major stages. First, the study area and temperature dataset are

described. Second, the data preprocessing procedures are presented. Third, the assumptions underlying EVT, particularly stationarity and independence, are assessed. Fourth, annual block maxima are extracted and modelled using the Generalized Extreme Value (GEV) distribution. Finally, exceedances above carefully selected thresholds are modelled using the Generalized Pareto Distribution (GPD). The estimation procedures, threshold diagnostics, goodness-of-fit assessment, and return-level analysis are presented in the subsequent sections.

2.1. Study area

The study was conducted in Namibia, a country located in the south-western region of Africa. Namibia covers an area of approximately 824 290 km^2 and possesses a coastline of about 1 572 km bordering the South Atlantic Ocean [3]. The country is characterised by an arid to semi-arid climate, with substantial spatial and temporal variability in temperature and rainfall. Climatic conditions are largely influenced by the cold Benguela Current along the western coastline, regional atmospheric circulation patterns, and subtropical high-pressure systems, resulting in considerable differences in temperature characteristics between coastal and inland regions [3, 6, 7, 8]. To capture these climatic contrasts, data was obtained from the Namibia Meteorological Service (NMS) and initially included records from five stations: Ondangwa, Keetmanshoop, Rundu, Windhoek and Walvis Bay. However, due to insufficient long-term temperature records from some stations, the analysis focused on three stations only, namely:

- Walvis Bay (coastal region),
- Windhoek (central highland region), and
- Rundu (northern inland region).

These stations represent distinct climatic conditions across Namibia, and their geographical distribution allows the assessment of regional variability in extreme high-temperature behaviour. Figure 1 shows the regions where the selected stations are located.

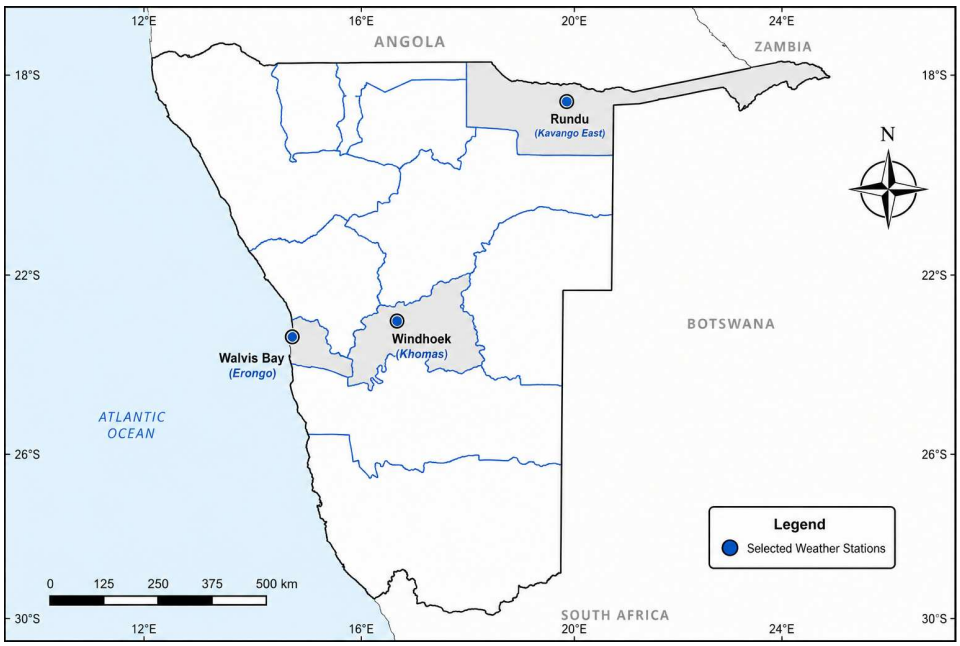


Figure 1: Map of Namibia showing the geographical locations of the selected weather stations used in this study: Walvis Bay (Erongo Region), Windhoek (Khomas Region), and Rundu (Kavango East Region).

2.2. Data Description and Preprocessing for Extreme-Value Analysis

Daily maximum air temperature observations for the period 1990-2019 were obtained from NMS, providing a sufficiently long observational record for EVT. The maximum daily temperatures are recorded in degrees Celsius (°C). In this study, the analysis focused exclusively on daily maximum temperatures, minimum temperatures, and lower-tail extremes is not considered. Before statistical analysis, the dataset was examined for completeness, consistency, and possible recording errors. Missing observations, duplicate records, and obvious data-entry errors were identified using standard quality-control procedures. Appropriate preprocessing of climate data is essential before extreme value theory (EVT) analysis, as the reliability of parameter estimates and return-level estimates depends critically on the quality and consistency of the underlying observations [26, 27]. The preprocessing included the following steps,

1. Initial data inspection: Raw daily maximum temperature records were examined for missing observations, duplicate records, invalid dates, and apparent transcription or recording errors.
2. Physical plausibility screening: Observations were screened against physically and climatologically plausible temperature ranges for the study region. For example, exceptionally high values such as 60°C were flagged for further investigation rather than automatically classified as extremes or errors.
3. Investigation and treatment of suspect observations: Suspect observations were removed or corrected only where there was sufficient evidence of a measurement, recording, or data-processing error. This distinction is particularly important in EVT, since statistically unusual observations may represent genuine extreme events and therefore should not be discarded solely because they appear as outliers [10, 9].
4. Temporal consistency checks: The observations were arranged chronologically and examined for temporal inconsistencies and implausibly large day-to-day changes in temperature. Where daily minimum temperature records were available, the consistency condition $T_{\max} \geq T_{\min}$ was also verified.
5. Assessment of data completeness: The temporal coverage and completeness of each station record were examined to identify periods with substantial missing observations that could affect the representation of annual extremes. Periods failing the predefined data-quality criteria were excluded from extreme-value analysis (e.g. Walvis Bay data for 1990-1993 and Windhoek data for 2018-2019 were missing therefore, they were excluded from the analysis).
6. Construction of the analysis series: After a good quality control [27], the retained daily maximum temperature observations were used to construct the samples required for the EVT analysis. In particular, annual block maxima for the BM approach were extracted, while threshold exceedances were identified for the POT approach.

Table 1: Summary statistics of daily maximum temperature ($^{\circ}C$) observations for the three meteorological stations from 1990 to 2019.

Station	Period	Available	Missing	Missing (%)	Mean	SD	Min	Max
Walvis Bay	Mar 1994–Jul 2019	8631	545	5.94	24.6	4.7	1	43.5
Windhoek	Jan 1990–Dec 2017	9794	281	2.79	27.6	4.4	8.5	38.7
Rundu	Jan 1990–Oct 2019	10619	355	3.23	31.1	3.8	16.6	41.0

Only observations that met the predefined criteria were retained for analysis. In addition, daily observations were evaluated against the annual completeness criterion, and years that did not meet

the criterion were excluded from the annual block-maxima series. A year was considered eligible for the annual BM analysis only when at least 90% of the expected daily observations for that year were available. Let n_y denote the number of available daily observations in year y and let N_y denote the expected number of daily observations in that year, accounting for leap years. The annual completeness ratio was calculated as

$$C_y = \frac{n_y}{N_y} \times 100,$$

where C_y represents the percentage of observations available in year y. Only years satisfying $C_y \geq 90\%$ were retained for the BM analysis.

2.3. Assessment of Stationarity and Independence

Classical EVT assumes that observations are approximately independent and identically distributed and that the underlying stochastic process is stationary throughout the period of analysis [9, 26]. Violations of these assumptions may introduce bias into parameter estimation and consequently affect return-level estimates [26]. Before fitting the GEV and GPD models, we examined the annual maximum temperature series for the presence of long-term monotonic trends to assess the validity of the stationarity assumption underlying classical EVT models. Stationarity was evaluated using the non-parametric Mann-Kendall trend test together with Sen's slope estimator [28]. The Mann-Kendall test is widely used in hydro-climatological studies because it does not require the data to follow a specific probability distribution and is relatively robust to outliers and missing observations [28, 29]. Let $\{x_1, x_2, \ldots, x_n\}$ denote the observed annual maximum temperature series. The Mann-Kendall test statistic is computed as [29]

$$S = \sum_{i=1}^{n-1} \sum_{j=i+1}^{n} \operatorname{sgn}(x_j - x_i), \tag{2.1}$$

where n is the total number of data points, and

$$\operatorname{sgn}(x) = \begin{cases} 1, & x > 0, \\ 0, & x = 0, \\ -1, & x < 0. \end{cases} \tag{2.2}$$

Under the null hypothesis of no monotonic trend, the expected value of S is zero. For sufficiently large samples ($n > 10$), the standardized test statistic is

$$Z = \begin{cases} \dfrac{S-1}{\sqrt{\operatorname{Var}(S)}}, & S > 0, \\ 0, & S = 0, \\ \dfrac{S+1}{\sqrt{\operatorname{Var}(S)}}, & S < 0, \end{cases} \tag{2.3}$$

where $\operatorname{Var}(S)$ denotes the variance of the Mann-Kendall statistic [28]. Positive values of Z indicate increasing trends while negative Z values show decreasing trends. At the 5% significance level, the null hypothesis of stationarity is rejected whenever $|Z| > 1.96$, indicating a statistically significant monotonic trend in the annual maximum temperature series. To quantify the magnitude of the detected trend, Sen's slope estimator was computed as

$$Q = \operatorname{median}\left(\frac{x_j - x_i}{j - i}\right), \qquad 1 \leq i < j \leq n. \tag{2.4}$$

A positive value of Q indicates an increasing trend in annual maximum temperatures, while a negative value indicates a decreasing trend [29]. The results of the Mann-Kendall test and Sen's slope estimator are presented in the result section and are used to assess the suitability of applying stationary EVT models to the observed temperature series.

2.3.1. Dependence considerations

For the Block Maxima (BM) analysis, the temporal dependence of the daily maximum temperature series was examined using the sample autocorrelation function (ACF) [30]. The ACF was evaluated over a sequence of temporal lags and compared with the approximate 95% significance limits to assess the presence of serial dependence. The resulting dependence diagnostics were considered when constructing the annual block maxima used in the GEV analysis. In contrast, for the Peaks Over Threshold (POT) analysis, the GPD was fitted directly to the observed daily exceedances above the selected threshold. No declustering procedure was applied; consequently, all identified exceedances were retained for GPD estimation. The resulting POT parameter estimates and return levels therefore correspond to the observed threshold exceedances without adjustment for possible temporal clustering.

2.4. Block Maxima approach

The Block Maxima (BM) approach involves dividing the observation period into non-overlapping blocks of equal duration, after which only the maximum observation from each block is retained for analysis. In this study, annual blocks were considered. Let $X_1, X_2, \ldots, X_n$ denote identically independent observations within a given year. The annual block maximum for each block of size n is defined as, $M_n = \max(X_1, X_2, \ldots, X_n)$. Assuming independence in the sequence $(X_1, \ldots, X_n)$, the underlying distribution of the block maximum is

$$\Pr(M_n \leq y) = \Pr(X_1 \leq y, \ldots, X_n \leq y) = \prod_{i=1}^{n} \Pr(X_i \leq y) = F^n(y) \tag{2.5}$$

where $F^n(y)$ denotes the cumulative distribution function of X_i. According to Fisher and Tippett [9] if there exist sequences of normalizing constants $\mu_n \in \mathbb{R}$ and $\sigma_n > 0$ such that the normalised block maxima converges

$$\Pr\left(\frac{M_n - \mu_n}{\sigma_n} \leq y\right) \to G(y) \quad \text{as} \quad n \to \infty \tag{2.6}$$

for all $y \in \mathbb{R}$, then $G(y)$ is a member of the Generalized Extreme Value (GEV) family [10, 9]

$$G(y) = \exp\left\{-\left[1 + \xi\left(\frac{y-\mu}{\sigma}\right)\right]^{-1/\xi}\right\}, \tag{2.7}$$

where $1 + \xi\left(\frac{y-\mu}{\sigma}\right) > 0$. Here, $\mu \in \mathbb{R}$ is the location parameter, $\sigma > 0$ is the scale parameter, and $\xi \in \mathbb{R}$ is the shape parameter. The value of the shape parameter determines the tail behaviour of the distribution. $\xi > 0$ corresponds to the Fréchet family (heavy tail); $\xi = 0$ corresponds to the Gumbel family (light tail); and $\xi < 0$ corresponds to the Weibull family (bounded upper tail). The fitted GEV models were then used to estimate return levels and return periods for extreme temperatures at each meteorological station.

2.5. Maximum likelihood estimation for the GEV model

The parameters of the GEV models were estimated using the Maximum Likelihood Estimation (MLE) method[**?**]. Let $M_1, M_2, \ldots, M_m$ be the annual block maxima extracted from the observed daily maximum temperatures. For the GEV distribution, the log-likelihood function is [**?**]

$$\ell(\mu,\sigma,\xi) = -m\log(\sigma) - \left(1+\frac{1}{\xi}\right)\sum_{i=1}^{m}\log\left[1+\xi\left(\frac{M_i-\mu}{\sigma}\right)\right] - \sum_{i=1}^{m}\left[1+\xi\left(\frac{M_i-\mu}{\sigma}\right)\right]^{-1/\xi}, \quad (2.8)$$

where,

$$1+\xi\left(\frac{M_i-\mu}{\sigma}\right) > 0, \qquad \sigma > 0.$$

The unknown parameters μ, σ, ξ were numerically estimated by maximizing the log-likelihood function in (2.8). The return time or return level is the average period, measured in years, expected between successive occurrences of an event [9, 26]. In practical terms, it indicates the average time expected between the occurrence of an event of a given intensity.The level of temperature return z_p is expressed by the following quantile function [9, 26],

$$z_p(T) = \begin{cases} \mu - \frac{\sigma}{\xi}\left[\{-\log(1-p)\}^{-\xi} - 1\right], & \xi \neq 0, \\ \mu - \sigma\log\{-\log(1-p)\}, & \xi = 0, \end{cases} \quad (2.9)$$

where $p = \frac{1}{T}$. Thus, for example $p = 0.1$ corresponds to a 10-year return period. The estimated return levels $\bar{z}_p$, which are the maximum temperatures expected for the return times T, are obtained by replacing the maximum likelihood estimates of the parameters in (2.9).

2.6. Peaks Over Threshold Approach

The Peaks Over Threshold (POT) approach provides an alternative to the Block Maxima method by retaining all observations that exceed a sufficiently high threshold rather than selecting only the maximum observation within each block [19]. Let X denote a daily maximum temperature and u denote a sufficiently high threshold. For observations exceeding u, the excess above the threshold is defined as

$$Y = X - u, \qquad X > u,$$

where $Y \geq 0$ represents the amount by which an observation exceeds the threshold u. The conditional distribution function of the excesses above u is defined as

$$F_u(y) = \Pr(X - u \leq y \mid X > u) = \frac{F(u+y) - F(u)}{1 - F(u)}, \qquad y \geq 0. \quad (2.10)$$

According to the Pickands-Balkema-de Haan theorem [19**?**], for a sufficiently high threshold u, the conditional excess distribution in (2.10) converges to a Generalized Pareto Distribution (GPD) function ,

$$H(y) = 1 - \left(1+\frac{\xi y}{\sigma_u}\right)^{-1/\xi}, \qquad \xi \neq 0, \quad (2.11)$$

subject to

$$y \geq 0, \qquad \sigma_u > 0, \qquad 1 + \frac{\xi y}{\sigma_u} > 0. \quad (2.12)$$

When $\xi = 0$, the limiting form of the GPD is the exponential distribution, therefore, equation 2.11 reduces to

$$H(y) = 1 - \exp\left(-\frac{y}{\sigma_u}\right). \quad (2.13)$$

The shape parameter ξ controls the upper-tail behaviour of the distribution. A positive value of ξ indicates a heavy or regularly varying upper tail, $\xi = 0$ corresponds to an exponential-type tail, and $\xi < 0$ indicates a bounded upper tail [19]. Unlike the Block Maxima approach, the POT method uses multiple threshold exceedances and can therefore provide greater statistical efficiency when an appropriate threshold is selected and the dependence structure of the exceedances is adequately addressed [19, 10, 13, 14, 17].

2.7. Threshold Selection for the POT Model

The selection of the threshold is a critical component of the POT approach because the choice of u determines both the number of exceedances and the validity of the asymptotic GPD approximation [19]. A threshold that is too low may result in substantial bias because the GPD approximation may not yet be valid, whereas a threshold that is too high results in very few exceedances and leads to an increases in the variance of the parameter estimates. Rather than selecting the threshold solely from visual inspection of the temperature series, an objective threshold-selection procedure was adopted in this study. A range of candidate thresholds was first considered for each meteorological station. The candidate thresholds were selected from sufficiently high empirical quantiles of the daily maximum temperature distribution [19]. For each candidate threshold, the following diagnostics were examined. First, the Mean Residual Life (MRL) plot was constructed. For a candidate threshold u, the empirical mean excess function is defined as

$$e(u) = E[X - u \mid X > u].$$

The empirical estimate is given by

$$\widehat{e}(u) = \frac{1}{N_u} \sum_{i:X_i>u} (X_i - u),$$

where N_u denotes the number of observations that exceed u. Second, parameter stability plots were constructed by fitting the GPD over a sequence of candidate thresholds. Third, threshold sensitivity analysis was conducted by comparing the estimates of the GPD parameters, goodness-of-fit statistics, and the number of exceedances across neighbouring candidate thresholds. The final threshold for each station was selected by jointly considering the MRL plot, the stability of the estimated GPD shape and scale parameters, and the number of exceedances available for model estimation. A threshold was deemed appropriate when the mean residual life (MRL) plot was approximately linear and the GPD parameter estimates remained stable across neighbouring thresholds. Among such candidates, preference was given to the lowest threshold that retained a sufficiently large number of exceedances while excluding observations below the range where the asymptotic GPD approximation is expected to hold. For a selected threshold u, the number of exceedances is defined as

$$N_u = \sum_{i=1}^{n} I(X_i > u), \qquad \text{where} \qquad I(X_i > u) = \begin{cases} 1, & X_i > u, \\ 0, & X_i \le u. \end{cases}$$

The selected threshold, the corresponding number and proportion of exceedances, and threshold-selection diagnostics are reported in Section 3.

2.8. Maximum Likelihood Estimation for the GPD Model

The same as for GEV, the parameters for the GPD were estimated using the MLE. Let $Y_1, Y_2, \ldots, Y_k$ denote the excesses above the selected threshold u, where

$$Y_i = X_i - u, \qquad X_i > u.$$

In the GPD model, the log-likelihood function for the scale parameter σ_u and shape parameter ξ, for $\xi \neq 0$, is

$$\ell(\sigma_u, \xi) = -k \log(\sigma_u) - \left(1 + \frac{1}{\xi}\right) \sum_{i=1}^{k} \log\left(1 + \frac{\xi Y_i}{\sigma_u}\right), \tag{2.14}$$

where

$$\sigma_u > 0, \qquad 1 + \frac{\xi Y_i}{\sigma_u} > 0, \qquad i = 1, \ldots, k.$$

For $\xi = 0$, the limiting exponential model has the log-likelihood

$$\ell(\sigma_u) = -k \log(\sigma_u) - \frac{1}{\sigma_u} \sum_{i=1}^{k} Y_i. \tag{2.15}$$

The unknown parameters σ_u and ξ were estimated numerically by maximizing the appropriate log-likelihood subject to the parameter constraints. The resulting estimates are denoted by $\hat{\sigma}_u$ and $\hat{\xi}$.

Return-level analysis for the POT was used to quantify the magnitude of extreme temperatures associated with specified return periods. Let $\lambda_u = \Pr(X > u)$ denote the probability that a daily maximum temperature exceeds the selected threshold. If exceedances occur at an average rate ζ_u per year, the POT return level associated with a return period T years is obtained from the GPD tail model [19]. For $\xi \neq 0$, the return level is given by

$$z_T = u + \frac{\sigma_u}{\xi} \left[(T\zeta_u)^{\xi} - 1 \right], \tag{2.16}$$

where ζ_u denotes the average number of threshold exceedances per year. Equivalently, if N_u exceedances are observed over N_y years, then

$$\widehat{\zeta}_u = \frac{N_u}{N_y}.$$

For the special case $\xi = 0$, the return-level expression becomes

$$z_T = u + \sigma_u \log(T\zeta_u). \tag{2.17}$$

The return level z_T therefore represents the temperature magnitude expected to be exceeded, on average, once every T years under the fitted POT model [10, 30]. Uncertainty in the estimated parameters and return levels was quantified using a non-parametric bootstrap procedure. The exceedance observations were resampled with replacement and the GPD parameters were re-estimated for each bootstrap sample. A total of $B = 2000$ bootstrap replications were used. For each bootstrap replication b, the parameter estimates $\hat{\sigma}_u^{(b)}$ and $\hat{\xi}^{(b)}$ were obtained, followed by the corresponding return-level estimates $z_T^{(b)}$. Bootstrap uncertainty intervals were preferred because the sampling distribution of the GPD shape parameter and long-period return levels can be substantially non-normal, particularly for relatively small samples [19].

2.9. Model Diagnostics and Goodness-of-Fit Assessment

The adequacy of the fitted GPD models was assessed using graphical and formal statistical diagnostics. Graphical diagnostics included (Q-Q) plots, (P-P) plots, empirical-versus-fitted distribution comparisons, and return-level plots. These diagnostics were used to determine whether the fitted GPD adequately represented the observed upper-tail behaviour of the temperature data [19]. Formal goodness-of-fit statistics were also calculated, including the Kolmogorov-Smirnov (KS), Cramér-von

Mises (CvM), and Anderson-Darling (AD) statistics, where applicable. Particular attention was given to the AD diagnostic because it places greater emphasis on discrepancies in the tails of the distribution. In addition, the fitted GEV and GPD models were also compared across candidate thresholds using the Akaike Information Criterion (AIC) and Bayesian Information Criterion (BIC). These criteria are defined as

$$AIC = -2\ell + 2k,$$

and

$$BIC = -2\ell + k\log(n),$$

where ℓ is the maximized log-likelihood, k is the number of estimated parameters, and n is the number of observations used in fitting the model. Smaller AIC and BIC values indicate a better complexity-adjusted fit when models are fitted to the same observations under comparable modelling conditions [**?**].For the final POT model at each station, the estimated GPD parameters, confidence intervals, number of exceedances, goodness-of-fit statistics, AIC, BIC, and return-level estimates are reported in Section 3.

3. Results and Discussions

3.1. Data characteristics and quality assessment

For each station, the observation dates were first checked for consistency and the daily maximum temperature records were examined for missing values. The number and proportion of available and missing observations are presented in Table 1. The number of daily observations available differs among the three stations, reflecting differences in data availability during the study period. The Walvis Bay station has the largest proportion of missing observations, whereas Rundu has the most complete record. Following the data-quality assessment, annual maximum daily temperatures were extracted from each station for all years for which temperature observations were available. The resulting Block Maxima series contained 26 annual maxima for Walvis Bay station (1994-2019), 28 annual maxima for Windhoek station (1990-2017), and 30 annual maxima for Rundu station (1990-2019) (Table 2). The shorter series for Walvis Bay and Windhoek resulted from the absence of observations during 1990-1993 and 2018-2019, respectively. No values were imputed for these missing years. Thus, the available annual maxima used in the GEV analysis are based exclusively on observed temperatures from years that satisfy the predefined completeness criterion.

Table 2: Summary of valid years and annual maxima (AM) of daily maximum temperature used for GEV modelling, by station.

Station	Valid years	Mean AM (°C)	SD (°C)	Min AM (°C)	Max AM (°C)
Walvis Bay	26	39.4	4.65	36.3	43.5
Windhoek	28	36.9	4.39	34	38.7
Rundu	30	39.4	3.82	37.2	41

3.2. Trend analysis of annual maximum temperatures

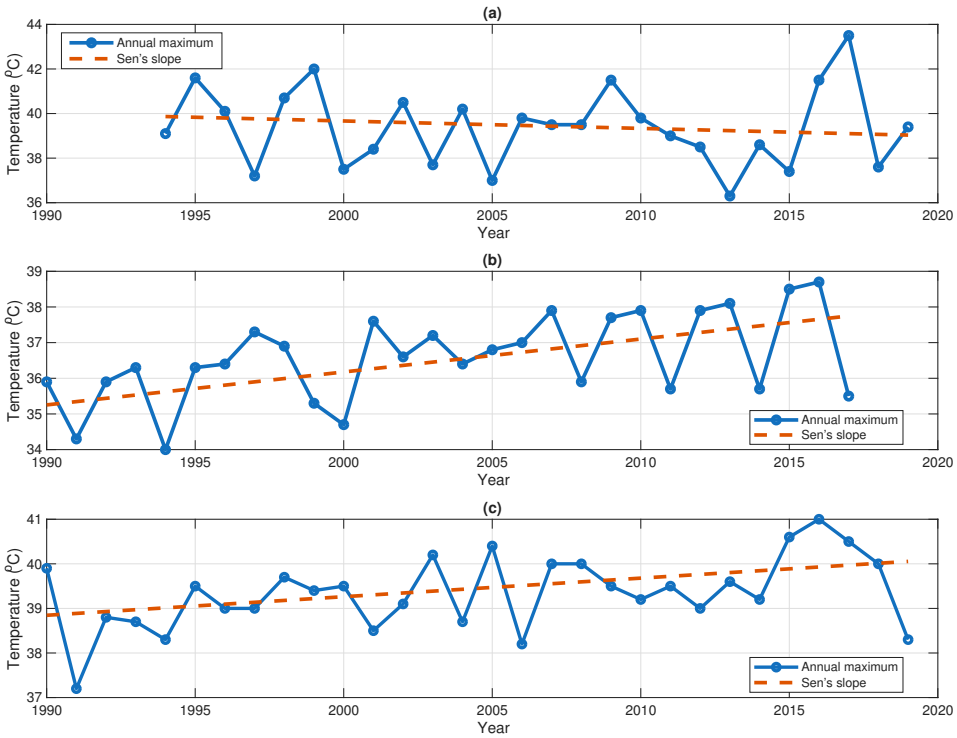
The temporal evolution of annual maximum temperatures was assessed using the Mann-Kendall test, while Sen's slope estimator was used to quantify the magnitude and direction of the observed trends. The analysis was performed separately for each station because the available observation periods differed among stations. The Walvis Bay series covered 1994-2019 ($n = 26$), Windhoek covered 1990-2017 ($n = 28$), and Rundu covered 1990-2019 ($n = 30$). The results is presented in

Table 3, indicating substantial spatial differences in the temporal behaviour of annual maximum temperatures. At Walvis Bay, the Mann-Kendall statistic was $S = -34$, with a standardized test statistic of $Z = -0.728$ and a corresponding p-value of 0.467. Thus, there was no statistically significant monotonic trend at the 5% significance level. As shown in Table 3, the estimated Sen's slope was $-0.0333\,^{\circ}\mathrm{C}$ per year, with a 95% confidence interval of $[-0.1550, 0.0818]\,^{\circ}\mathrm{C}$ per year. Because the confidence interval includes zero, the estimated negative slope does not provide sufficient evidence of a systematic decrease in annual maximum temperatures during the study period. In contrast, Windhoek exhibited a statistically significant increasing trend with the Sen's slope estimate of $0.0923\,^{\circ}\mathrm{C}$ per year, with a 95% confidence interval of $[0.0429, 0.1300]\,^{\circ}\mathrm{C}$ per year. This corresponds to an estimated increase of approximately $0.92\,^{\circ}\mathrm{C}$ per decade in annual maximum temperature over the observation period. Similarly, a statistically significant increasing trend was also detected at Rundu station ($p = 0.0253 < 0.05$), with the estimated Sen's slope was $0.0417\,^{\circ}\mathrm{C}$ per year, and a 95% confidence interval of $[0.0036, 0.0778]\,^{\circ}\mathrm{C}$ per year, corresponding to an increase of approximately $0.42\,^{\circ}\mathrm{C}$ per decade.

Table 3: Mann–Kendall trend test and Sen's slope estimates using $\alpha = 0.05$. MK (s) = Mann–Kendall statistic, Sen's (s) = Sen's slope (°C/year)

Station	n	MK (s)	Z	p-value	Sen's (s)	95% CI	Interpretation
Walvis Bay	26	-34	-0.728	0.467	-0.0333	[-0.1550, 0.0818]	No significant trend
Windhoek	28	149	2.930	0.0034	0.0923	[0.0429, 0.1300]	Significant increasing trend
Rundu	30	126	2.237	0.0253	0.0417	[0.0036, 0.0778]	Significant increasing trend

Figure 2: Mann-Kendall trend analysis of daily maximum temperatures at (a) Walvis Bay, (b) Windhoek, and (c) Rundu stations.



As visualised in Figure 2 the trend analysis indicates that the temporal behaviour of annual maximum temperatures is not spatially uniform across the three stations. While no statistically significant

monotonic trend was detected at the coastal Walvis Bay station, significant increasing trends were observed at the inland stations of Windhoek and Rundu. These results are important for the EVT analysis because the assumption of stationarity may not be appropriate for all stations. Accordingly, both stationary and, where supported by the data, non-stationary extreme-value specifications are considered in the subsequent analysis.

3.3. Temporal dependence of annual maximum temperatures

Before fitting the Block Maxima-Generalized Extreme Value models, the temporal dependence structure of the annual maximum temperature series was examined using the sample autocorrelation function (ACF) and the Ljung-Box test. The ACF was evaluated for lags of up to five years, while the Ljung-Box test was conducted at lags 1, 2, 3, and 5 years using a significance level of $\alpha = 0.05$. Figure 3 presents the ACF results, which reveal relatively small correlations across the three stations. As shown in Figure 3, Walvis Bay and Rundu stations indicated no evidence of persistent autocorrelation pattern, while Windhoek has a relatively noticeable lag-3 correlation. To test whether the series contains statistically significant serial correlation, the Ljung-Box test was conducted. As shown in Tabale 4, results provided no statistically significant evidence of serial dependence at the 5% significance level. Therefore, the null hypothesis of no serial correlation was not rejected for any of the tested lags at any station. These findings provide empirical support for treating the annual block maxima as approximately independent for the purposes of the BM analysis. However, because the POT analysis is based on daily threshold exceedances, temporal dependence among consecutive exceedances was assessed separately using a declustering procedure.

Figure 3: Autocorrelation of annual maximum temperatures at different lags for each station. (a) Walvis Bay station, (b) Windhoek station and (c) Rundu station

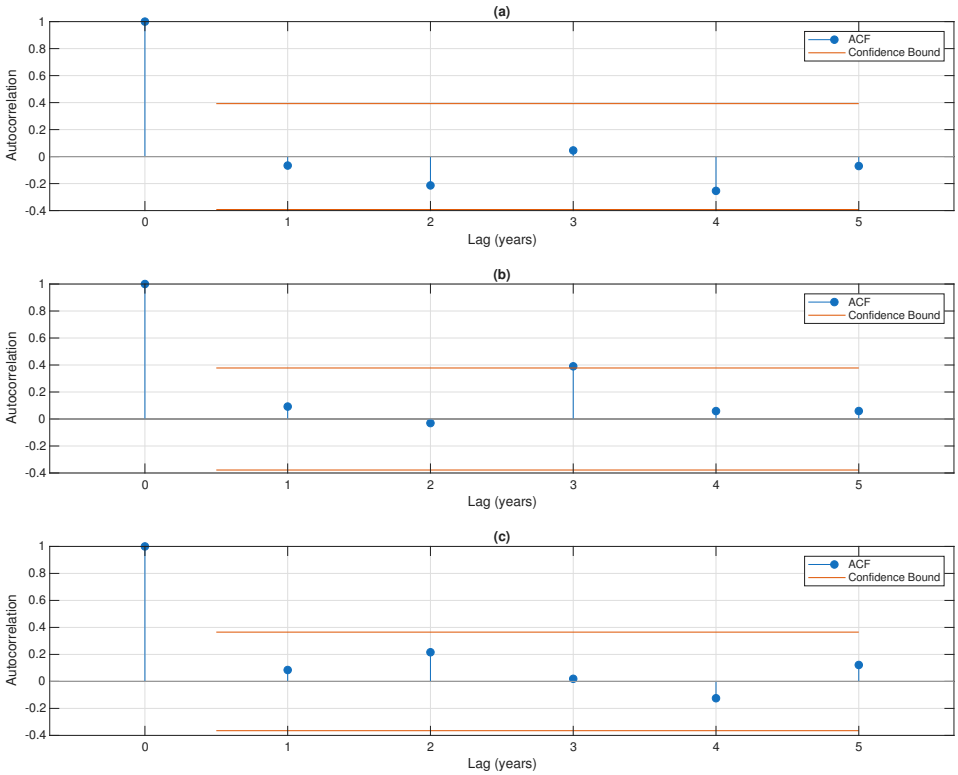


Table 4: Ljung-Box test results for autocorrelation at different lags for each station.

Station	Lag	Q	p-value	Decision at $\alpha = 0.05$
Walvis Bay	1	0.128	0.720	No dependence
	2	1.511	0.470	No dependence
	3	1.577	0.665	No dependence
	5	3.879	0.567	No dependence
Windhoek	1	0.264	0.607	No dependence
	2	0.294	0.863	No dependence
	3	5.413	0.144	No dependence
	5	5.661	0.340	No dependence
Rundu	1	0.237	0.627	No dependence
	2	1.835	0.399	No dependence
	3	1.848	0.604	No dependence
	5	2.992	0.701	No dependence

3.4. Block Maxima and Generalized Extreme Value Results

The BM approach was applied to the annual maximum daily temperatures recorded at Walvis Bay, Windhoek, and Rundu. After accounting for the availability of observations at each station, 26 annual maxima were available for Walvis Bay, 28 for Windhoek, and 30 for Rundu. The corresponding annual maximum temperatures ranged from 36.3°C to 43.5°C at Walvis Bay, from 34.0°C to 38.7°C at Windhoek, and from 37.2°C to 41.0°C at Rundu. The GEV distribution was fitted separately to the annual maximum series at each station using MLE. The estimated location parameter ($\hat{\mu}$), scale parameter ($\hat{\sigma}$), and shape parameter ($\hat{\xi}$), together with their 95% bootstrap confidence intervals, are reported in Table 5. A total of 2,000 bootstrap replicates were generated for each station, and all bootstrap replications successfully converged.

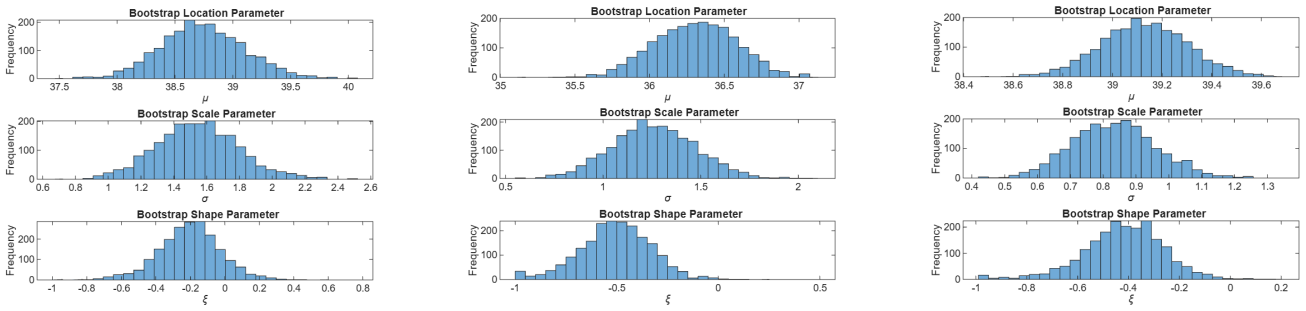
Table 5: GEV parameter estimates, uncertainty intervals, model fit statistics, and goodness-of-fit measures for annual maximum temperatures with 95% confidence interval.

Station	N (Years)	$\hat{\mu}$	$\hat{\sigma}$	$\hat{\xi}$	LogLik	AIC	BIC
Walvis Bay	26	38.687	1.601	-0.176	-50.783	107.565	111.339
Windhoek	28	36.260	1.282	-0.450	-44.145	94.291	98.288
Rundu	30	39.098	0.849	-0.370	-36.028	78.056	82.260

The estimated location parameters indicate clear differences in the central levels of annual extreme temperatures among the three stations, with Rundu having the highest estimate ($\hat{\mu} = 39.098$°C), followed by Walvis Bay ($\hat{\mu} = 38.687$°C) and Windhoek ($\hat{\mu} = 36.260$°C). Walvis Bay exhibited the largest GEV scale parameter, indicating greater variability in annual temperature extremes, whereas Rundu had the smallest scale parameter. The shape parameter was negative at all three stations, indicating a Weibull-type GEV tail and a finite upper endpoint under the fitted stationary model. Thus, the fitted models provide no evidence of a heavy-tailed upper distribution of annual maximum temperatures. The 95% confidence interval for the shape parameter at Walvis Bay included zero,

suggesting that its tail behaviour cannot be distinguished statistically from the Gumbel case at the 5% significance level. In contrast, the confidence intervals for Windhoek and Rundu excluded zero, providing stronger evidence of bounded upper tails at these stations.

To further assess parameter uncertainty, bootstrap distributions of the GEV location, scale, and shape parameters were obtained and are presented in Figure 4. The bootstrap results provide an indication of the sampling variability of the parameter estimates, with greater dispersion reflecting higher uncertainty. This is particularly relevant for the shape parameter, which is generally more sensitive to the limited number of annual block maxima available for estimation. The corresponding AIC and BIC values were calculated using the same three-parameter GEV model for each station (Table 5), allowing the fitted models to be compared based on their station-specific datasets.



(a) Walvis Bay station (b) Windhoek station (c) Rundu station

Figure 4: Bootstrap distributions of the GEV location, scale, and shape parameters for the three meteorological stations.

3.4.1. Goodness-of-fit and model diagnostics

The KS, CvM, and AD statistics are reported in Table 6. The KS test produced statistics of 0.103, 0.091, and 0.081 for Walvis Bay, Windhoek, and Rundu, respectively. The corresponding p-values were 0.918, 0.958, and 0.979.

Table 6: Goodness-of-fit statistics for the fitted GEV models.

Station	KS statistic	KS p-value	CvM statistic	AD statistic
Walvis Bay	0.1032	0.9180	0.0276	0.1966
Windhoek	0.0911	0.9579	0.0318	0.2046
Rundu	0.0813	0.9794	0.0244	0.1697

At the 5% significance level, the KS test does not reject the fitted GEV distribution for any of the three stations. The relatively small KS statistics and large p-values suggest that, according to this test, there is no statistically significant deviation from the fitted GEV distributions. The CvM and AD statistics were also relatively small across all stations, providing additional graphical and distributional diagnostics in support of the fitted models. These results are visualized in the Q–Q, P–P, and density plots presented in Figures 5–7.

3.4.2. Estimated return levels

The fitted GEV models was further examined through return-level analysis. The estimated return levels and their 95% bootstrap confidence intervals for all stations are presented in Table 7.

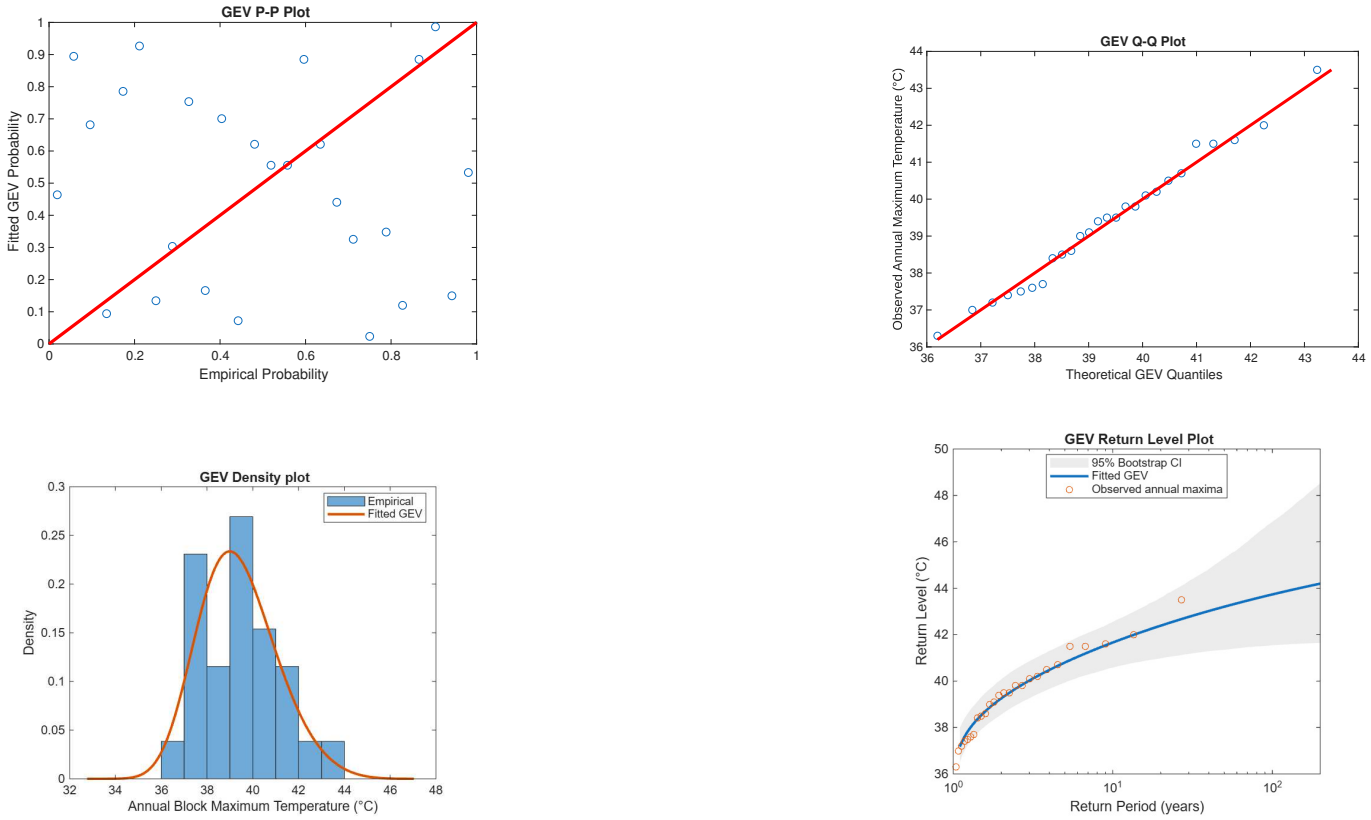


Figure 5: Diagnostic plots for GEV distribution fitted to annual maximum temperatures for Walvis Bay station.

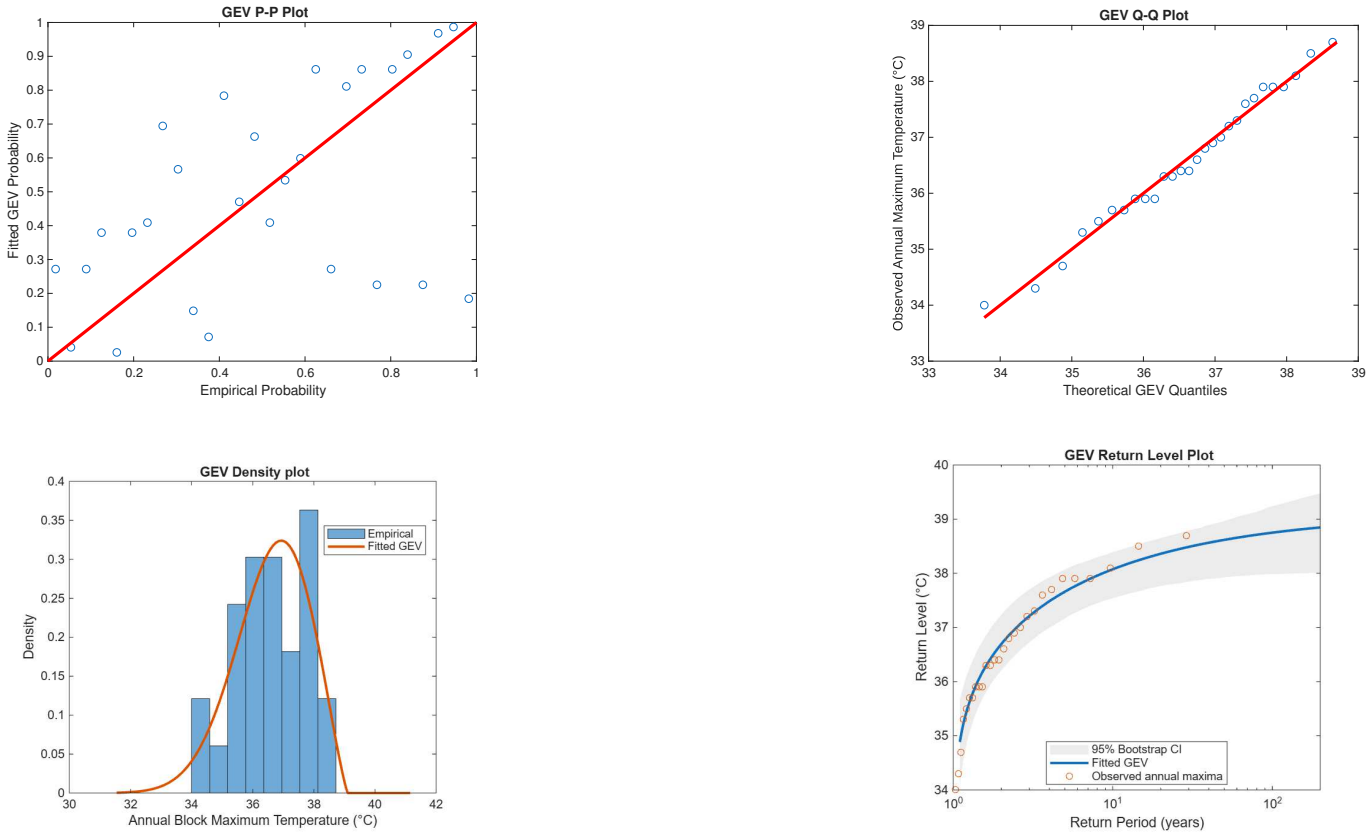


Figure 6: Diagnostic plots for GEV distribution fitted to annual maximum temperatures for Windhoek station.

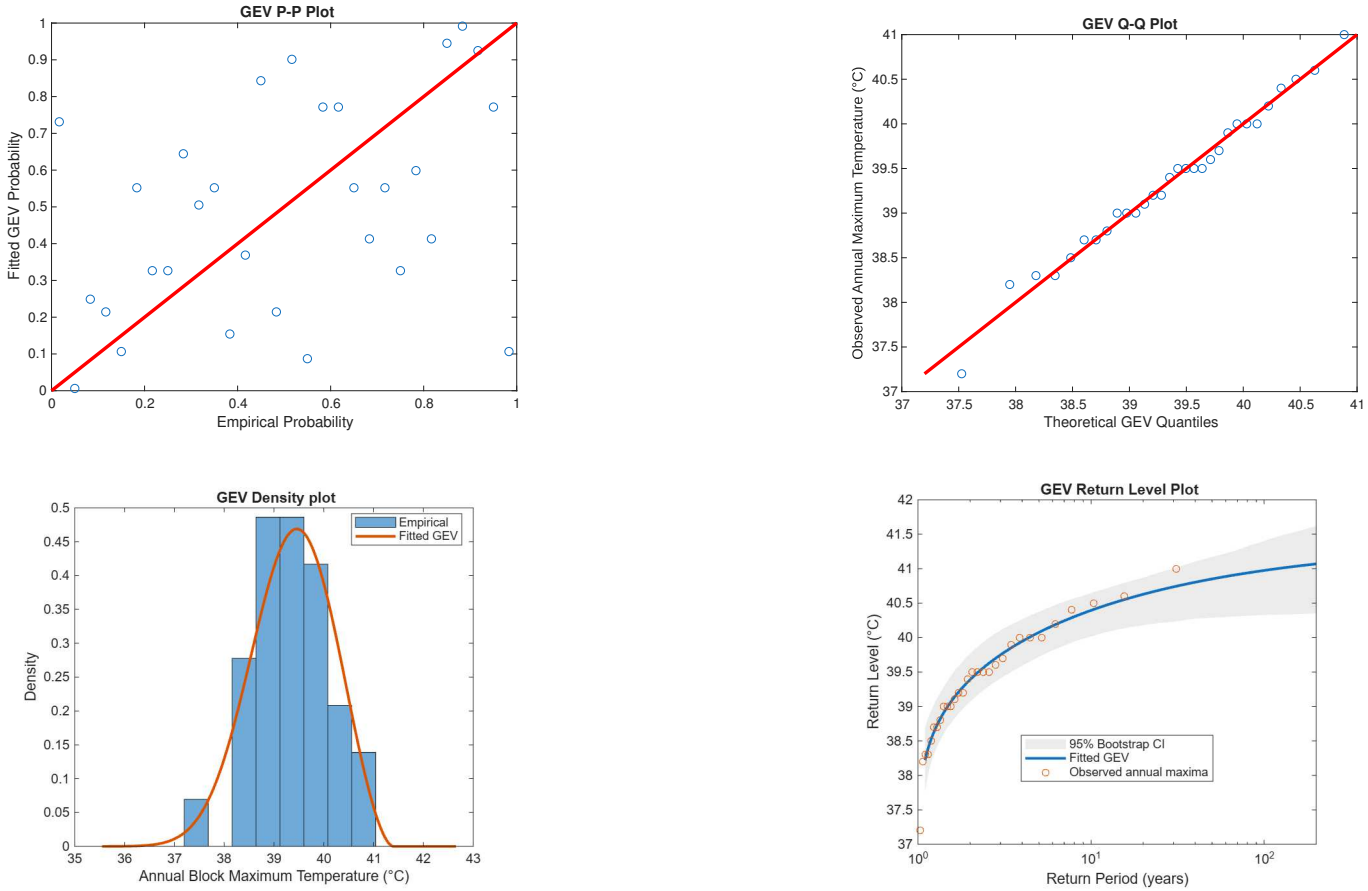


Figure 7: Diagnostic plots for GEV distribution fitted to annual maximum temperatures for Rundu station.

At Walvis Bay, the corresponding uncertainty intervals widened substantially for the longer return periods, with the 100-year return-level interval extending from 41.546°C to 46.860°C. This widening reflects the greater uncertainty associated with estimating events whose return periods substantially exceed the effective length of the observed record. For Windhoek, the estimated return level increased from 36.693°C for two-year to 38.750°C for the 100-year return period. The relatively small increase between the longer return periods is consistent with the negative estimated shape parameter and the corresponding bounded-tail behaviour of the fitted GEV model. Similar to Windhoek, the increment between the 50- and 100-year return levels for Rundu was relatively small, which is consistent with the estimated negative shape parameter.

The return-level results indicate distinct station-level differences in the magnitude of extreme annual temperatures. Walvis Bay produced the largest estimated upper return levels, particularly for return periods of 20 years and longer, whereas Windhoek produced the lowest return levels. Rundu exhibited intermediate return levels, although its 10-year and 100-year estimates remained higher than those of Windhoek. These differences are descriptive of the station-specific temperature distributions and should not, by themselves, be interpreted as evidence of a causal climatic mechanism. The return-level curves and their corresponding uncertainty bands are shown in Figures 5–7. The increasing return levels across all stations demonstrate that larger annual maximum temperatures are associated with progressively longer return periods under the fitted stationary GEV models. However, the widening uncertainty bands, particularly for the 50-year and 100-year return periods, indicate that extrapolation beyond the 30-year observational period should be interpreted with caution.

3.5. Peaks Over Threshold results (GPD)

Table 7: Estimated GEV return levels (°C) and 95% bootstrap confidence intervals for selected return periods.

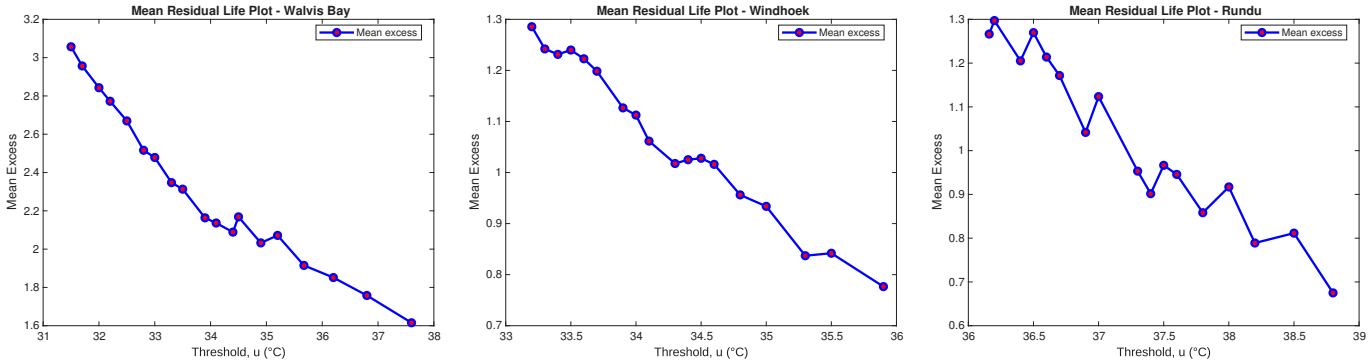
Station	Return period (yr)	Return level	Lower CI	Upper CI
Walvis Bay	2	39.256	38.559	40.075
	5	40.798	39.934	41.618
	10	41.662	40.582	42.551
	20	42.389	40.984	43.591
	50	43.204	41.350	45.296
	100	43.733	41.546	46.860
Windhoek	2	36.693	36.210	37.235
	5	37.659	37.163	38.068
	10	38.075	37.541	38.389
	20	38.361	37.765	38.651
	50	38.617	37.925	38.962
	100	38.750	37.985	39.238
Rundu	2	39.389	39.069	39.765
	5	40.075	39.722	40.372
	10	40.395	40.017	40.648
	20	40.628	40.179	40.869
	50	40.851	40.289	41.172
	100	40.974	40.329	41.402

The POT analysis for each station was performed based on the available daily observations (Table 1). The final thresholds were 34.4°C, 34.3°C, and 37.3°C for Walvis Bay, Windhoek, and Rundu, respectively. These thresholds yielded 374, 458, and 502 exceedances, corresponding to approximately 4.33%, 4.68%, and 4.73% of the available daily maximum-temperature observations. The threshold diagnostics, including the mean residual life and parameter stability plots, indicated adequate stability around the selected thresholds (Figures 8-11).

Table 8: Selected thresholds, number of exceedance (N_u) and estimated parameters of the GPD with 95% CI for the POT analysis.

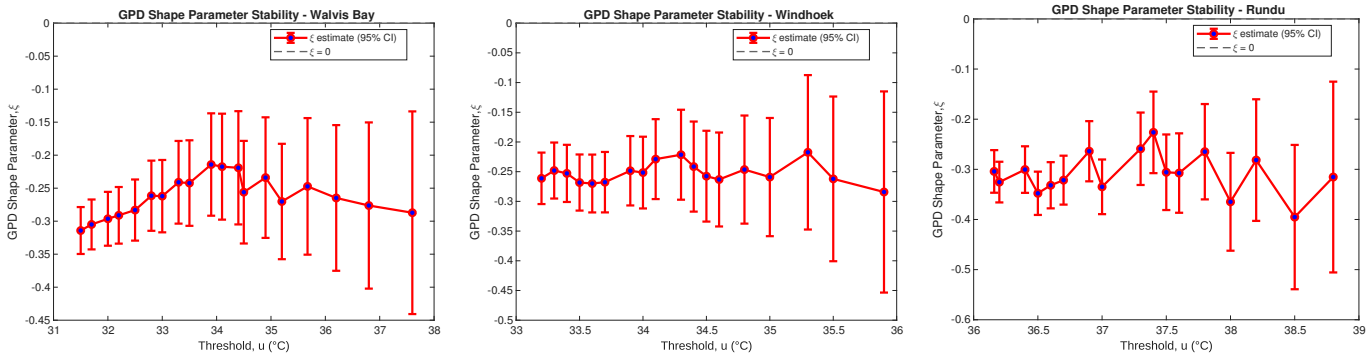
Station	u (°C)	N_u (%)	Exceedance/yr	Mean Excess	$\hat{\xi}$ (95% CI)	$\hat{\sigma}_u$ (95% CI)
Walvis Bay	34.4	374 (4.33)	14.38	2.0888	-0.2191(-0.34,-0.14)	2.55 (2.25,2.93)
Windhoek	34.3	458 (4.68)	16.36	1.0177	-0.2215(-0.31,-0.16)	1.24 (1.11,1.40)
Rundu	37.3	502 (4.73)	16.73	0.9532	-0.2590(-0.32,-0.20)	1.199 (1.08,1.34)

The fitted GPD parameter estimates are presented in Table 8. The estimated scale parameters were 2.5503, 1.2428, and 1.1994°C for Walvis Bay, Windhoek, and Rundu, respectively. The corresponding shape parameters were -0.2191, -0.2215, and -0.2590. The 95% bootstrap confidence intervals for the shape parameter excluded zero at all three stations. This suggests a consistently bounded upper tail for the distribution of temperature exceedances. The bootstrap intervals also



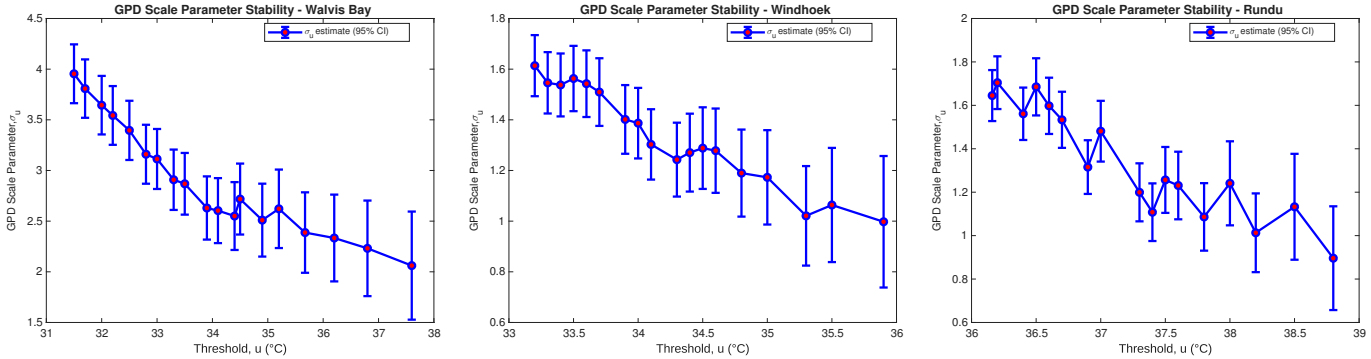
(a) Walvis Bay station (b) Windhoek station (c) Rundu station

Figure 8: Mean residual life plots for the three meteorological stations.



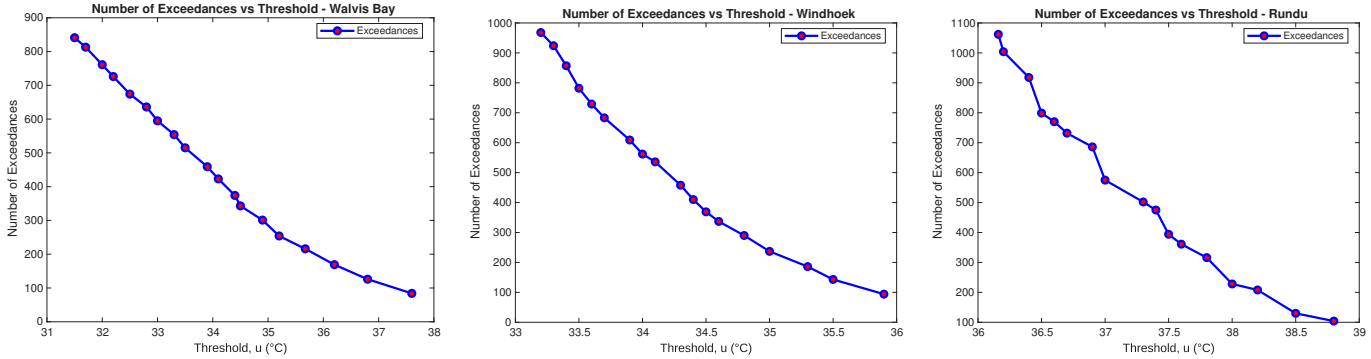
(a) Walvis Bay station (b) Windhoek station (c) Rundu station

Figure 9: Shape stability plots for the three meteorological stations.



(a) Walvis Bay station (b) Windhoek station (c) Rundu station

Figure 10: Scale stability plots for the three meteorological stations.



(a) Walvis Bay station (b) Windhoek station (c) Rundu station

Figure 11: Scale stability plots for the three meteorological stations.

indicate relatively precise estimation of the GPD scale parameters. The fitted models provided a good fit to the exceedances at Walvis Bay with $p = 0.4616$, while for Windhoek and Rundu, the KS tests indicated departures from the fitted GPD at the 5% significance level with $p < 0.001$. The corresponding CvM and AD statistics are also reported in Table 9. These results suggest that the GPD provides the most adequate representation of the observed threshold exceedances at Walvis Bay, while the fits for Windhoek and Rundu should be interpreted with greater caution.

Table 9: Goodness-of-fit statistics for the fitted GPD models.

Station	KS	KS p-Value	CvM	AD	LogLik	AIC	BIC
Walvis Bay	0.044273	0.46162	0.078499	0.88193	-642.2	1288.4	1296.2
Windhoek	0.077978	0.0076221	0.19305	2.1782	-456.14	916.28	924.53
Rundu	0.10294	4.7909e-05	0.63127	5.1963	-463.25	930.5	938.94

The diagnostic plots (Figures 12, 13, and 14) indicate a reasonable agreement between the fitted GPD distributions and the observed threshold exceedances, although the degree of agreement varies among stations. For all three stations, the P-P show close agreement between the empirical and fitted probabilities and Q-Q plots show that the empirical and theoretical quantiles are generally aligned, particularly over the central range of the exceedance distributions. The density comparisons indicate that the fitted GPDs capture the main distributional pattern of the observed exceedances. The corresponding CDF plots (Figure 15) provide a similar assessment, with the fitted cumulative distributions generally following the empirical distributions. These graphical results are broadly consistent with the numerical goodness-of-fit statistics reported in Table 9. In particular, the Walvis Bay fit provides the strongest overall agreement, whereas the Windhoek and Rundu fits exhibit greater departures in the tail behaviour. Nevertheless, the negative shape estimates for all three stations indicate a bounded upper tail, implying that the fitted extreme-temperature distributions have a finite upper limit.

The estimated return levels are given in Table 10 and illustrated in Figures 12, 13, and 14. At Walvis Bay, the estimated return level increases from 40.46°C for a 2-year return period to 43.67°C for a 100-year return period. The corresponding estimates for Windhoek increase from 37.32°C to 38.82°C, while those for Rundu increase from 40.065°C to 41.254°C. The confidence intervals get wider for longer return periods because there is more uncertainty when predicting events beyond the observed range of threshold exceedances.

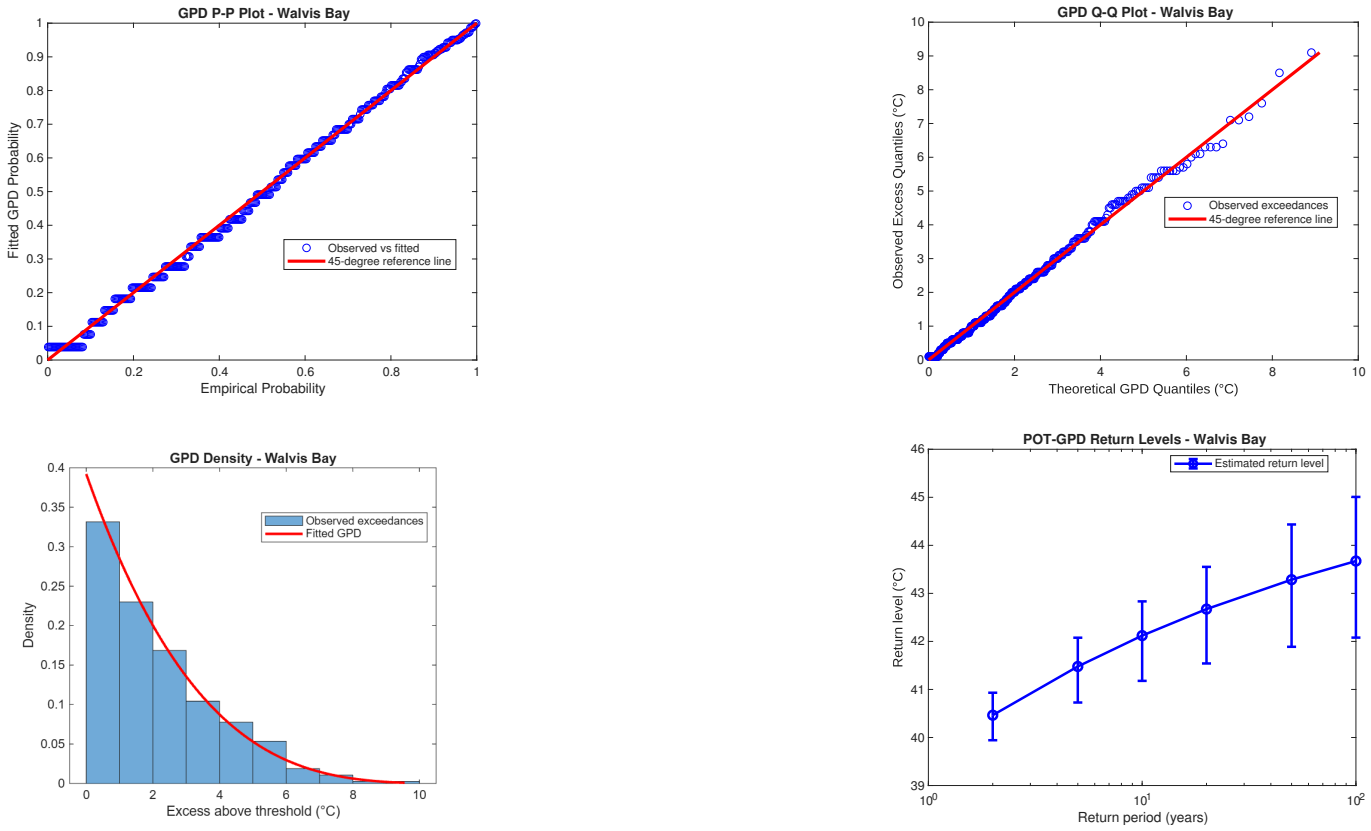


Figure 12: Diagnostic plots for the GDP distribution fitted to the exceedances at Walvis Bay.

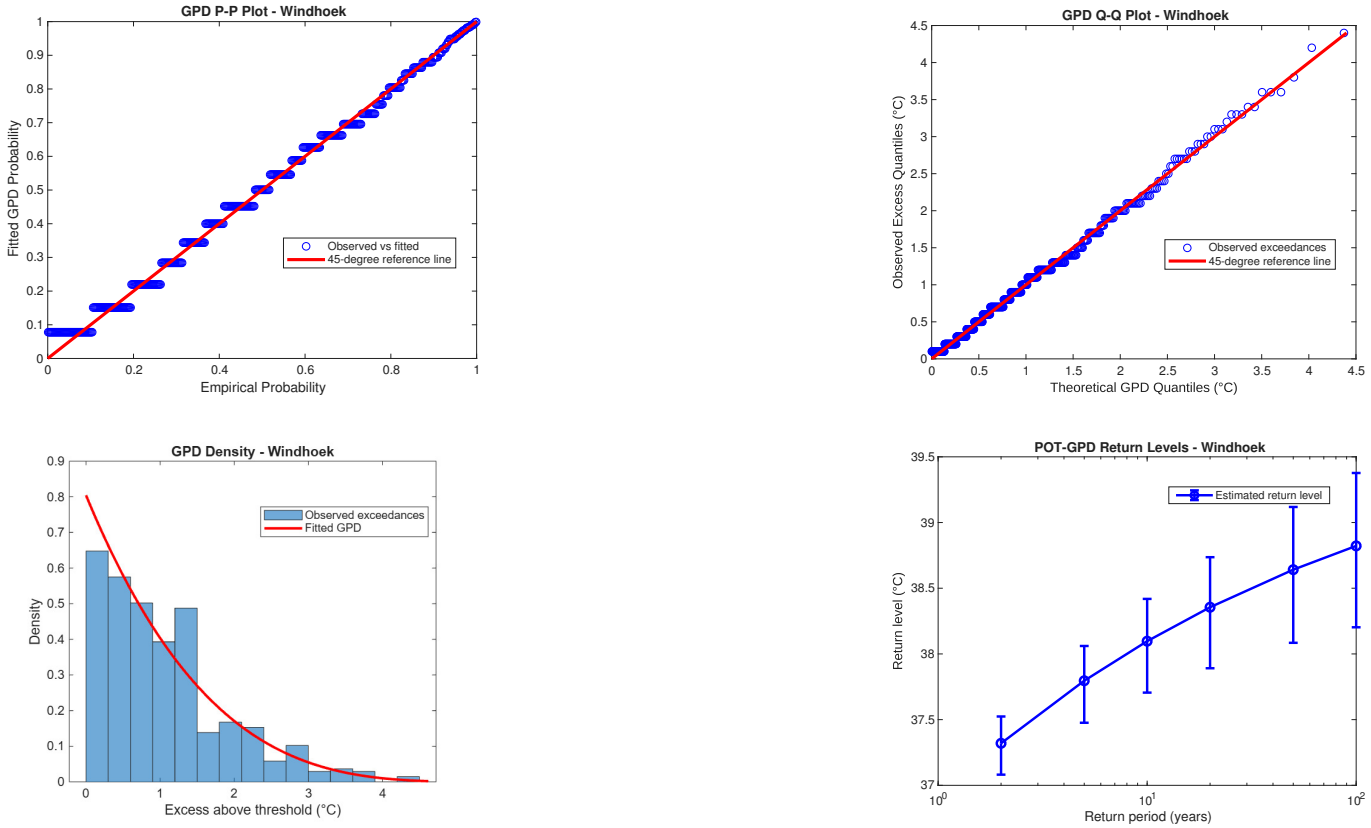


Figure 13: Diagnostic plots for the GDP distribution fitted to the exceedances at Windhoek.

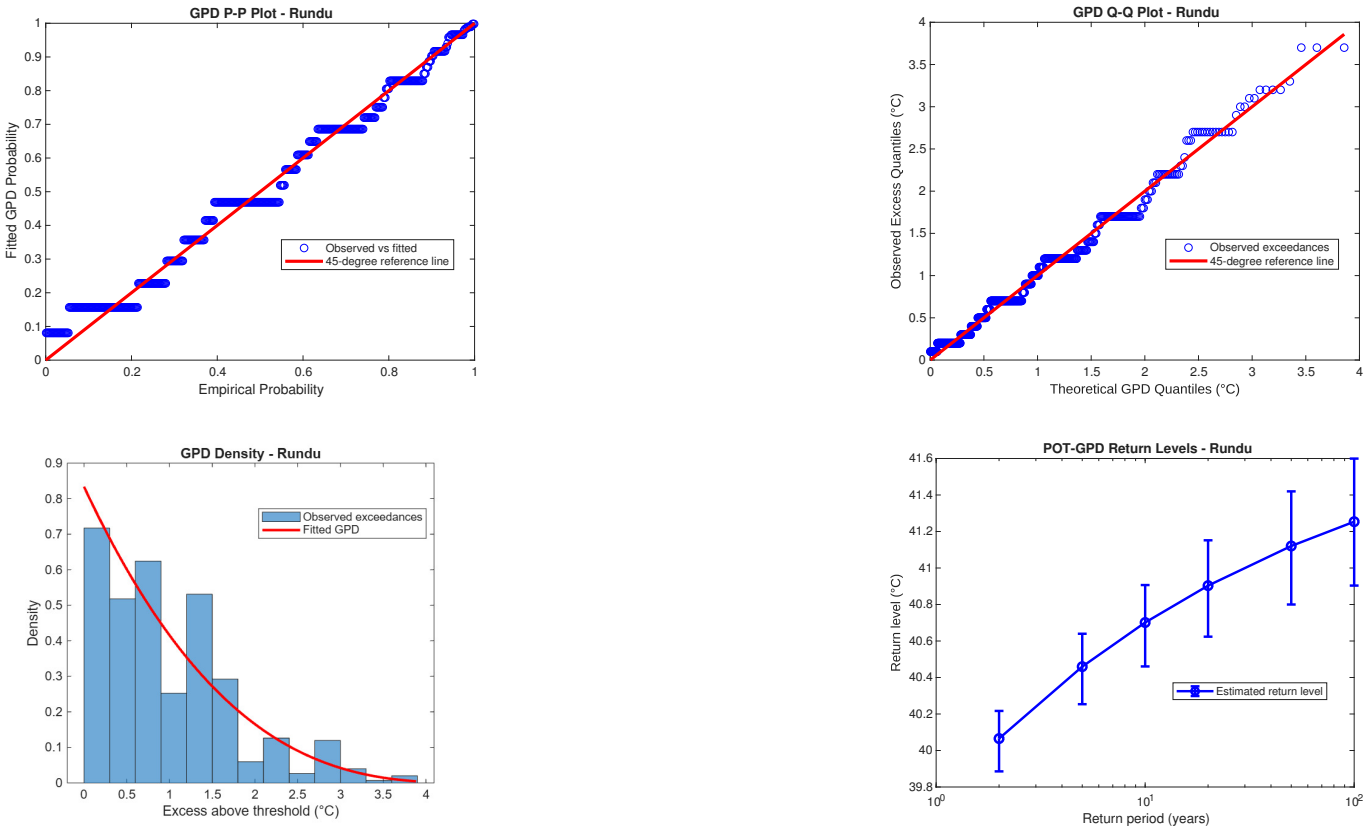
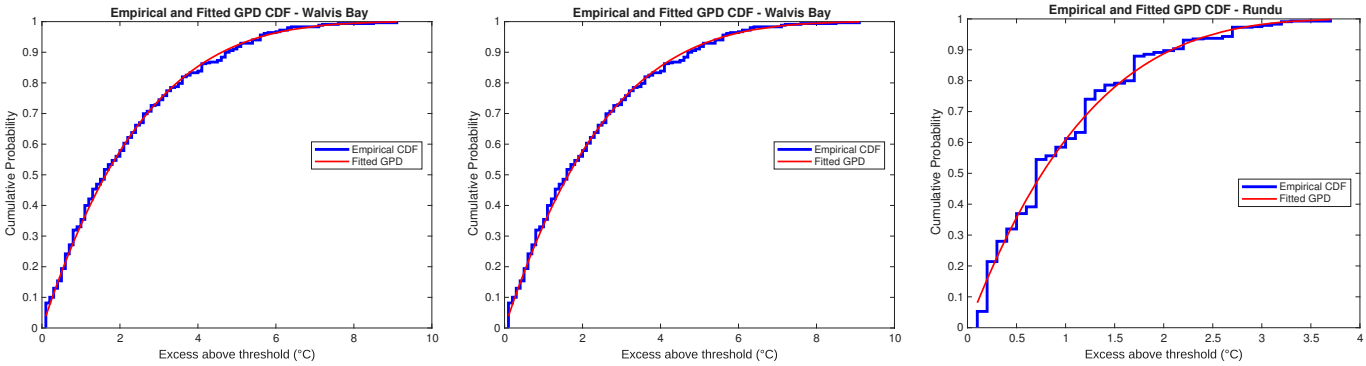


Figure 14: Diagnostic plots for the GDP distribution fitted to the exceedances at Rundu.



(a) Walvis Bay station (b) Windhoek station (c) Rundu station

Figure 15: Empirical and fitted cumulative distribution functions for the GPD threshold exceedances at Walvis Bay, Windhoek, and Rundu.

Table 10: Estimated GPD return levels, 95% confidence intervals for selected return periods.

Station	Return Period (yr)	Return Level	Lower CI	Upper CI
Walvis Bay	2	40.464	39.943	40.932
	5	41.478	40.728	42.077
	10	42.121	41.179	42.833
	20	42.673	41.541	43.552
	50	43.285	41.888	44.435
	100	43.673	42.079	45.008
Windhoek	2	37.32	37.081	37.524
	5	37.796	37.476	38.06
	10	38.097	37.706	38.419
	20	38.355	37.891	38.736
	50	38.641	38.085	39.118
	100	38.822	38.203	39.377
Rundu	2	40.065	39.886	40.217
	5	40.46	40.254	40.64
	10	40.701	40.461	40.907
	20	40.903	40.624	41.152
	50	41.121	40.8	41.42
	100	41.254	40.904	41.599

3.6. Comparison of Extreme Temperature Behaviour Across Stations and EVT Models

The GEV and GPD analyses reveal distinct patterns in the magnitude and tail behaviour of extreme temperatures across Walvis Bay, Windhoek, and Rundu (Tables 5,6 ,8, 9, and 10). The GPD estimates show negative shape parameters at all three stations, with $\hat{\xi} = -0.2191$ for Walvis Bay, $\hat{\xi} = -0.2215$ for Windhoek, and $\hat{\xi} = -0.2590$ for Rundu, indicating bounded upper tails. Rundu shows the most negative shape parameter and therefore the strongest indication of a finite upper endpoint among the three stations. Comparison of the return-level estimates from the two EVT approaches provides further insight into the spatial and methodological differences in extreme temperature behaviour. The POT analysis gives the highest long-period return levels for Walvis Bay, increasing from 40.46°C for the 2-year return period to 43.67°C for the 100-year return period. Rundu follows, with return levels increasing from 40.07°C to 41.25°C, while Windhoek records substantially lower GPD-based return levels. The corresponding GEV estimates should be considered alongside these results to assess the sensitivity of projected extremes to the choice between the Block Maxima and POT frameworks. The comparison also highlights differences between coastal and inland locations. Although Windhoek and Rundu generally have higher typical temperatures than Walvis Bay, the POT results indicate higher estimated upper-tail extremes at Walvis Bay and Rundu than at Windhoek. The estimated exceedance rates are relatively similar, ranging from 14.38 events per year at Walvis Bay to 16.73 events per year at Rundu (Table 8), suggesting that differences in extreme-temperature risk are more pronounced in the magnitude of the extremes than in their annual exceedance frequency. The comparison demonstrates that both the geographical location and

the EVT models influence the estimated behaviour of extreme temperatures. The results therefore support the use of station-specific extreme-value assessments for heat-risk planning. In particular, the higher upper-tail temperatures projected for Walvis Bay and Rundu warrant attention in long-term heat-risk planning, while the significant goodness-of-fit departures for the Windhoek and Rundu GPD fits suggest that their long-period return-level estimates should be interpreted with appropriate caution

4. Conclusion

This study investigated the behaviour of extreme daily maximum temperatures at three meteorological stations in Namibia using two complementary Extreme Value Theory (EVT) approaches: the Block Maxima approach based on the Generalized Extreme Value (GEV) distribution and the Peaks Over Threshold (POT) approach based on the Generalized Pareto Distribution (GPD). The analysis examined the distribution and tail behaviour of temperature extremes and quantified the magnitude of rare events through return-level estimation. The GEV approach used annual maximum temperatures, while the POT approach incorporated a larger proportion of extreme observations exceeding carefully selected station-specific thresholds. Threshold selection was supported by mean residual life (MRL) plots, parameter stability and exceedance diagnostics, followed by maximum likelihood estimation of the GPD parameters. Model adequacy was evaluated using graphical diagnostics and formal goodness-of-fit measures, while bootstrap procedures were employed to quantify uncertainty in the estimated parameters and return levels.

The results demonstrate clear spatial differences in extreme-temperature behaviour across the three stations and show that the choice of EVT models can influence the estimated magnitude of rare events. The POT analysis produced negative GPD shape estimates at all stations, ranging from $\hat{\xi} = -0.2191$ at Walvis Bay to $\hat{\xi} = -0.2590$ at Rundu, indicating bounded upper-tail behaviour. The estimated 100-year return levels were 43.67°C for Walvis Bay, 38.82°C for Windhoek and 41.25°C for Rundu, demonstrating substantial spatial variation in the magnitude of rare temperature extremes. In contrast, the annual exceedance rates were relatively comparable, ranging from 14.38 to 16.73 exceedances per year, indicating that differences among stations are more evident in the magnitude of extreme temperatures than in the frequency of threshold exceedances. These findings demonstrate the usefulness of EVT for quantifying rare temperature extremes in Namibia and provide a statistical basis for station-specific heat-risk assessment. The complementary use of GEV and GPD provides a more comprehensive characterisation of temperature extremes, while the spatial differences identified across the stations highlight the importance of accounting for local climatic characteristics when assessing extreme heat. In general, the findings provide a statistical basis for understanding station-specific extreme-temperature behaviour and for informing future heat-risk assessment in Namibia.

4.1. Policy recommendations

The findings of this study have important implications for management of heat-risk and climate adaptation in Namibia. The station-specific return-level estimates provide quantitative information that can support the development and strengthening of heat-risk planning, early-warning systems, and climate adaptation strategies in areas vulnerable to extreme temperatures. Meteorological monitoring and early-warning mechanisms should be strengthened to facilitate timely communication of extreme heat risks to communities, health services, agriculture, water-resource managers and other climate-sensitive sectors. Such measures can contribute to improved preparedness and reduce the potential impacts of severe heat events.

As climate change continues to increase the pressure on climate-sensitive systems, sustained preparedness and adaptation will remain important for building resilience for Namibian communities. Although Namibia has made progress towards creating an enabling environment for climate-change

response, continued efforts are required to translate climate information into locally relevant risk-management actions. In particular, the spatial differences in extreme temperature behaviour identified in this study suggest that heat-risk planning should account for location-specific characteristics rather than relying on a uniform national threshold or risk profile.

4.2. Limitations and directions for future research

The present analysis was restricted to three meteorological stations and therefore does not fully represent the spatial variability of extreme temperatures across Namibia. Future studies should extend the analysis to additional stations and regions, incorporate longer and more complete temperature records where available, and also investigate the influence of climatic and environmental factors on the spatial and temporal variability of extreme temperatures. Such extensions would provide a more comprehensive basis for national-scale heat-risk assessment and climate adaptation planning.

Declarations

4.3. Funding

This research received no external funding.

4.4. Conflict of interest

The authors declare that they have no known competing financial interests or personal relationships that could have appeared to influence the work reported in this paper.

4.5. Ethical approval

Not applicable.

4.6. Consent to participate

Not applicable.

4.7. Consent to publish

Not applicable.

4.8. Clinical trial number

Not applicable.

4.9. Data availability

The data used in this study are available from the corresponding author upon reasonable request.

4.10. Author contributions

All authors contributed equally to the conception of the study, data analysis, interpretation of results, manuscript preparation, and revision. All authors read and approved the final manuscript.

References

[1] AghaKouchak, A., Chiang, F., Huning, L. S., Love, C. A., Mallakpour, I., Mazdiyasni, O., ... & Sadegh, M. (2020). *Climate extremes and compound hazards in a warming world*. Annual review of earth and planetary sciences, 48(1), 519-548..

[2] Heim Jr, R. R. (2015). An overview of weather and climate extremes–Products and trends. Weather and Climate Extremes, 10, 1-9.

[3] Dos Reis, C. J., Souza, A., Graf, R., Kossowski, T. M., Abreu, M. C., de Oliveira-Junior, J. F., & Fernandes, W. A. (2022). Modeling of the air temperature using the Extreme Value Theory for selected biomes in Mato Grosso do Sul (Brazil). *Stochastic Environmental Research and Risk Assessment*, 36(10), 3499-3516.

[4] Wambua, M. M., Mung'atu, J. K., and Aduda, J. A. (2020). Modelling extreme temperature using extreme value theory: A case study of Northern Kenya. *International Journal of Data Science and Analysis*, 6(5), 130-136.

[5] Horton, R. M., Mankin, J. S., Lesk, C., Coffel, E., & Raymond, C. (2016). A review of recent advances in research on extreme heat events. Current Climate Change Reports, 2(4), 242-259.

[6] Dirkx, E., Hager, C., Tadross, M., Bethune, S., and Curtis, B. (2008). *Climate Change Vulnerability and Adaptation Assessment*. Desert Research Foundation of Namibia and Climate Systems Analysis Group, prepared for the Ministry of Environment and Tourism, Namibia.

[7] Wilhelm, M. (2013). *Impact of Climate Change in Namibia: A Case Study of Omusati Region*. Doctoral dissertation.

[8] Somses, S., Bopape, M. J. M., Ndarana, T., Fridlind, A., Matsui, T., Phaduli, E., ... & Rakate, E. (2020). *Convection parametrization and multi-nesting dependence of a heavy rainfall event over Namibia with Weather Research and Forecasting (WRF) model*. Climate, 8(10), 112.

[9] Fisher, R. A., and Tippett, L. H. C. (1928). Limiting forms of the frequency distribution of the largest or smallest member of a sample. *Proceedings of the Cambridge Philosophical Society*, 24, 180-190.

[10] Winter, H. (2016). *Extreme Value Modelling of Heatwaves*. Doctoral dissertation, Lancaster University.

[11] Omondi, P. A. O., Awange, J. L., Forootan, E., Ogallo, L. A., Barakiza, R., Girmaw, G. B., and Kilavi, M. (2014). Changes in temperature and precipitation extremes over the Greater Horn of Africa region from 1961 to 2010. *International Journal of Climatology*, 34(4), 1262–1277.

[12] Wu, C., Xiao, L., Hu, Z., & Zhou, Y. (2022). Modeling the low-carbon behaviors' development paths of freight enterprises based on a survey in Zhejiang, China. *Sustainable Cities and Society*, 82, 103894.

[13] Hussain, F., Li, Y., Arun, A., & Haque, M. M. (2022). A hybrid modelling framework of machine learning and extreme value theory for crash risk estimation using traffic conflicts. *Analytic methods in accident research*, 36, 100248.

[14] Uwingabire, J. (2018). *Modelling Extreme Health Insurance Claims Using Generalized Pareto Distribution*. Master's dissertation, University of Rwanda, Kigali, Rwanda.

[15] Nuugulu, S. M., and Kock, G. (2020). On a loss distribution approach for allocating operational risk capital in banks. *Journal of Mathematical and Statistical Analysis*, 3, 101.

[16] Karpov, O. E., Grubov, V. V., Maksimenko, V. A., Kurkin, S. A., Smirnov, N. M., Utyashev, N. P., ... & Hramov, A. E. (2022). Extreme value theory inspires explainable machine learning approach for seizure detection. *Scientific Reports*, 12(1), 11474.

[17] Gumbel, E. J. (1958). *Statistics of Extremes*. New York: Columbia University Press.

[18] Lazoglou, G., and Anagnostopoulou, C. (2017). An overview of statistical methods for studying extreme rainfalls in the Mediterranean. In *Proceedings*, 1(5), 681. https://doi.org/10.3390/ecas2017-04132

[19] Coles, S. (2001). *An Introduction to Statistical Modeling of Extreme Values*. London: Springer.

[20] Garcia-Cueto, O. R., and Santillan-Soto, N. (2012). Modeling extreme climate events: Two case studies in Mexico. In *Climate Models*. IntechOpen.

[21] Kolaković, S., Mandić, V., Stojković, M., Jeftenić, G., Stipić, D., & Kolaković, S. (2023). Estimation of large river design floods using the peaks-over-threshold (POT) method. *Sustainability*, 15(6), 5573.

[22] Singirankabo, E., Iyamuremye, E., Habineza, A., & Nelson, Y. (2023). Statistical modelling of maximum temperature in Rwanda using extreme value analysis. *Open Journal of Mathematical Sciences (OMS)*, 7, 180-195.

[23] Chen, W., Zhao, X., Zhou, M., Chen, H., Ji, Q., & Cheng, W. (2024). Statistical inference and application of asymmetrical generalized Pareto distribution based on peaks-over-threshold model. *Symmetry*, 16(3), 365.

[24] Lee, J. (2022). *Bayesian analysis of nonstationary extremes*.

[25] Naftal, L., De Cauwer, V., & Strohbach, B. J. (2024). Potential distribution of major plant units under climate change scenarios along an aridity gradient in Namibia. *Vegetation Classification and Survey*, 5, 127-151.

[26] de Haan, L., and Ferreira, A. (2006). *Extreme Value Theory: An Introduction*. New York: Springer.

[27] Domonkos, P., Tóth, R., & Nyitrai, L. (2022). Climate observations: data quality control and time series homogenization (Vol. 3). Elsevier.

[28] Frimpong, B. F., Koranteng, A., & Molkenthin, F. (2022). Analysis of temperature variability utilising Mann–Kendall and Sen's slope estimator tests in the Accra and Kumasi Metropolises in Ghana. *Environmental Systems Research*, 11(1), 24.

[29] Abdulfattah, I. S., Rajab, J. M., Chaabane, M., & San Lim, H. (2025). Trend analysis of air surface temperature using Mann-Kendall test and Sen's slope estimator in Tunisia. *Journal of Agrometeorology*, 27(3), 355-359.

[30] Gedefaw, M. (2023). Assessment of changes in climate extremes of temperature over Ethiopia. *Cogent Engineering*, 10(1), 2178117.